Rain Drop Shapes and Scattering Calculations: A Case Study using 2D Video Disdrometer Measurements and Polarimetric Radar Observations at S-band During Hurricane Dorian Rain-Bands

Merhala Thurai[1], Sophie Steger[2], Franz Teschl[2], Michael Schönhuber[3], David B. Wolff[4]
[1] Department of Electrical and Computer Engineering, Colorado State University, Fort Collins, CO 80523, USA, merhala@colostate.edu
[2] Institute of Communication Networks and Satellite Communications, Graz University of Technology, 8010 Graz, Austria
[3] JOANNEUM RESEARCH Forschungsgesellschaft mbH, 8010 Graz, Austria
[4] NASA/GSFC, Wallops Flight Facility, Wallops, VA 23337, USA

***Abstract*— On 9 September 2019, rain-bands of category-1 Hurricane Dorian passed over a ground instrumentation site in Delmarva peninsula, USA. Drop shapes derived from 2D Video Disdrometer measurements at this site were used to compute the S-band radar cross sections (RCS) for horizontal and vertical polarizations for each drop with equi-volume diameter > 2 mm. These are combined with RCS for the smaller drops assuming equilibrium shapes. Radar reflectivity (Z_H) and differential reflectivity (Z_{DR}) are calculated for each of the 3 minutes throughout the event which lasted for more than 8 hours. These are compared with simultaneous observations from an S-band polarimetric radar 38 km away. The comparisons highlight the impact of large amplitude drop oscillations on Z_{DR}.**

***Index Terms*— rain drop shapes, 2D video disdrometer, S-band radar reflectivity, differential reflectivity.**

I. Introduction

Rain drop shapes play an important and a central role in evaluating radiowave propagation effects [1,2] for earth-space and terrestrial links as well as rainfall remote sensing by polarimetric radars [3, 4, 5]. In the former case, information on drop shapes are needed for evaluating rain attenuation effects and the polarization dependence as well as rain-induced depolarization effects, often expressed in terms of the variation of the cross-polar discrimination (XPD) with the co-polar attenuation (CPA) [6, 7]. For the latter case, they are needed for estimating rainfall rates and microphysical parameters more accurately [8] which have applications in hydrology and meteorological modelling respectively.

Our understanding of drop shapes for drop diameters > 2 mm is now on a firm footing from both precise wind-tunnel measurements [9] and from 2D-video disdrometer (2DVD) measurements [10] from the "80-m fall experiment" as reviewed in [11]. The most probable shapes derived from 2DVD in [10] have been shown to be in excellent agreement with the equilibrium numerical model of [12] well within their estimated error bounds. 2DVD measurements in natural rain have also been made but only a few cases had simultaneous observations from polarimetric radar, for example [13, 14].

In this paper, we examine 2DVD measurements during a category-1 Hurricane (Dorian) event whose rain-bands had traversed a ground instrumentation site located in Delmarva peninsula, USA. An S-band polarimetric radar, 38 km from the 2DVD site, had been used to perform continuous observations. The scan sequence included range-height indicator (RHI) scans over the disdrometer site.

Scattering calculations are performed on a drop-by-drop basis, and subsequently used to determine the S-band co-polar reflectivity (Z_H) and differential reflectivity (Z_{DR}) which in turn are compared with the radar observations. We draw an important conclusion from these comparisons.

II. The Rain Event, Measurements and Observations

Hurricane Dorian made landfall in the United States near the Florida coastline at the end of August 2019. It then moved along the east coast of the continent, later becoming a post-tropical cyclone. The rain-bands of the storm had traversed a site at the NASA Wallops Precipitation Research Facility [15] where a network of ground instruments including several 2DVDs had been installed. The site is within the coverage of NASA's S-band polarimetric radar, NPOL.

The event which occurred on 9 September 2019 lasted for more than 8 hours [16] and here we analyze 2DVD measurements and radar observations from 11:00 UTC to 19:00 UTC. The event had unusually large drops. Fig. 1 shows the 3-minute drop size distribution (DSD) for the 8-hour period. The color scale represents the drop concentration and the thick grey line represents the maximum recorded equi-volume drop diameter within each 3-minute interval. As can be seen drops larger than 5 mm were recorded several times and the largest drop that was recorded was 8.06 mm at 15:58 UTC. A study using microphysical simulations [17] together with radar observations of vertical profiles (especially of co-polar correlation coefficient, ρ_{hv}) over the 2DVD location had

clearly indicated that these were all fully melted hydrometeors (i.e. rain drops) at ground level. An example of an RHI scan of Z_H taken at 16:02 UTC is shown in Fig. 2(a) and the vertical profiles of Z_H, Z_{DR} and ρ_{HV} over the 2DVD are shown in Fig. 2(b), (c), and (d) respectively. Despite the presence of large drops at ground level, the RHI shows that it was stratiform rain as indicated by the radar bright-band seen clearly between 3.5 to 4 km height above ground level (representing the melting layer region). The vertical profile in panel (b) shows > 40 dBZ near ground level whereas panel (c) shows that the corresponding Z_{DR} is only about 1 dB. ρ_{HV} in panel (d) is very close to 1 below the melting layer down to ground level implying fully melted hydrometeors, especially close to ground. Note, due to beam blockage, radar data below 500 m (above ground level) need to be omitted from further consideration.

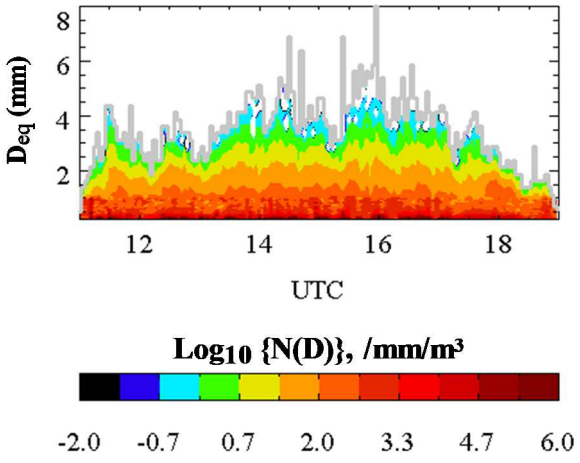

Fig. 1: DSD plot from 11:00 to 19:00 UTC

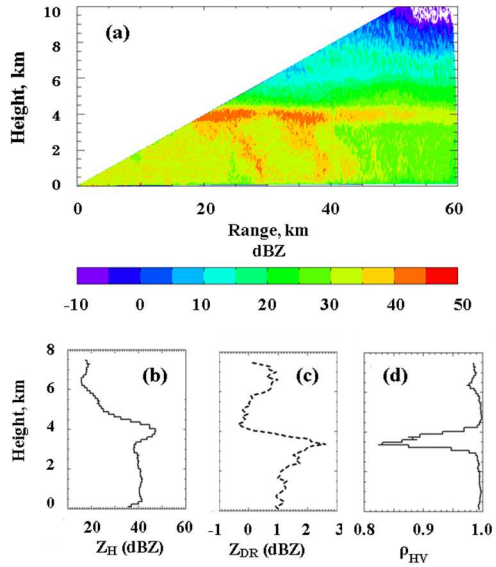

Fig. 2: (a) RHI scan taken along the azimuth of the 2DVD (at 16:02 UTC), with grey line showing the location; (b), (c) and (d) vertical profile of Z_H, Z_{DR} and ρ_{HV}.

III. Drop Shapes and Scattering Calculations

To reconstruct the drop shapes from the 2DVD images, we make use of the recorded contours of each drop in the two orthogonal planes. The procedure has been described previously [18,19,20] hence will not be repeated here, but one point to note is that, owing to a number of limitations, the shape reconstruction was only performed for relatively large drops, viz. for equi-volume drop diameter (D_{eq}) > 2 mm. An example of a reconstructed large drop is shown in Figure 3. Note the drop does not possess rotational symmetry. For smaller drops, we use the most probable shapes with rotational symmetry from [10].

The scattering calculation of each reconstructed drop has been carried out, using CST Studio Suite 2020, a 3D electromagnetic (EM) analysis software package that provides EM solvers for application across a wide frequency spectrum. For the required calculation of the radar cross section (RCS) of the raindrops at 2.8 GHz frequency, the built-in Integral Equation Solver has been used. The scattering calculations have been automatized by controlling CST via an application programming interface (API), scripted by Matlab code.

Fig. 4 shows an example of the reconstructed drop from Fig. 3, after importing into CST and after performing a surface triangulation. As material, the dielectric properties of water at 2.8 GHz frequency at a temperature of 20° C have been calculated by applying the formulae of Ray [21].

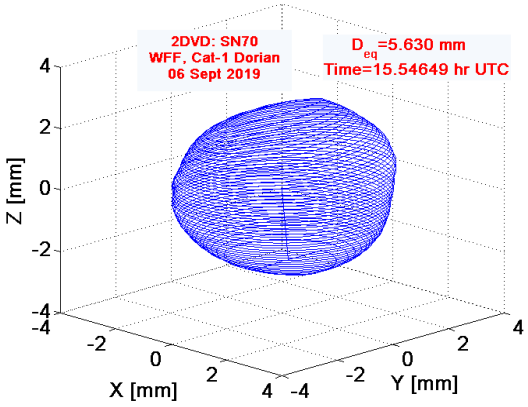

Fig. 3: An example of a reconstructed drop from the Dorian event

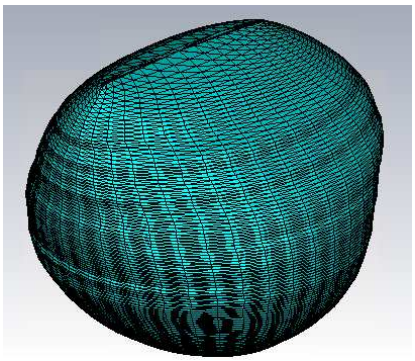

Fig. 4: Modelled drop in CST Studio Suite after surface triangulation.

Fig. 5 shows the simulated RCS of the example drop for both horizontal and vertical polarization, as a function of the horizontal view angle. Note for an equi-volume sphere this value would be -72.3 dBm² for all angles. Here we use the RCS values corresponding to the view angle from the radar.

IV. Calculations of Z_H and Z_{DR} and Comparisons with Radar Data

RCS values for H and V polarizations for each drop were used to compute Z_H and Z_{DR} over every 3 minute interval from 11:00 to 19:00 UTC using the same approach given in [13,14]. For around 5% of a total of 15202 drops > 2 mm, the reconstruction was not possible. For those drops (and for the drops ≤ 2 mm) the RCS values corresponding to the most-probable shapes were used. The radar reflectivity is calculated from the individual scattering amplitudes, for example over a 3-minute period, by performing drop-by-drop integration of the radar cross-sections (in actual fact the covariance matrix elements) during the specified time period. If the H-polarization reflectivity for the ith drop is denoted by z_i^h, then the overall reflectivity from all drops over the 3-minute time interval is:

$$Z_H = \frac{1}{A\Delta t}\sum_{i=1}^{n} v_i^{-1}\, z_i^h \qquad (1)$$

where v_i is the vertical (fall) velocity of the ith drop, A represents the measurement area of the 2DVD, and, Δt represents the averaging time period which in this case is 180 seconds. For V polarization, similar integration is performed using the corresponding RCS values, z_i^v. Both are converted to the conventional dBZ units and Z_{DR} for each of the 3-minute period is determined from the difference between the two.

The computed Z_H and Z_{DR} are shown as green points in Panels (a) and (b) of Fig. 6. These are compared with the NPOL radar data extracted over the 2DVD site shown as black lines. Because of the aforementioned beam blockage, data at a height of 500 meters have been used, and moreover, 3 pixels on either side (= 450 m) of the 2DVD site are included. Additionally, for Z_{DR}, a previously reported filtering technique was applied [16]. The unfiltered Z_{DR} are shown as grey points.

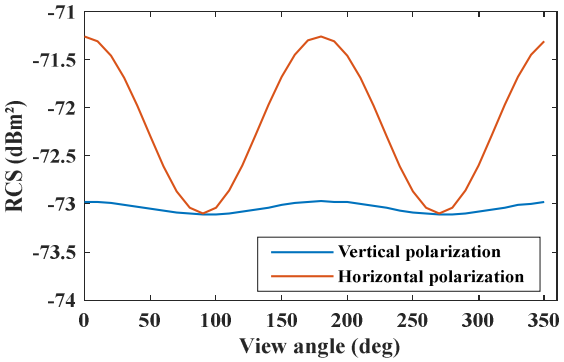

Fig. 5: Simulated RCS as a function of the horizontal view angle for the drop in Fig. 4 for horizontal and vertical polarization (2.8 GHz).

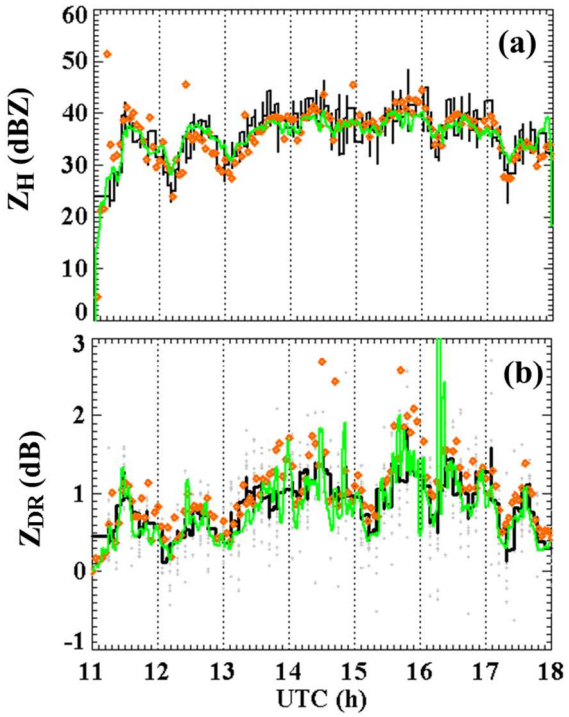

Fig. 6: (a) Z_H and (b) Z_{dr} calculations using individual drop shape scattering amplitudes (green lines) compared with NPOL data over the 2DVD site (black lines) and calculations using the most probable (or equilibrium) shapes. For panel (b), the grey points represent the unfiltered Z_{dr} from NPOL radar and the black line represents the filtered Z_{dr}.

Fig. 7 also shows the Z_H and Z_{DR} calculated using 3-minute DSDs assuming the most-probable (= equilibrium) shapes, represented by the orange points. Apart from a 9 minute time interval around 16:15 UTC, the green line shows better Z_{DR} agreement than the orange points, the latter tending to be higher than the Z_{DR} from NPOL. On the other hand, Z_H does not show any noticeable differences. Note radar calibration of Z_H and Z_{DR} was extensively performed throughout the event.

In Fig. 7, we show the variation of (unfiltered) Z_{DR} versus Z_H from NPOL (grey points) as well as those from the two sets of scattering calculations. They are all the same points as in Fig. 6. Also shown, as purple line, is the power-law fitted curve to the radar data. The better agreement with the green points is seen more clearly. The calculated relative bias (RB) had a mean of 1.9% for the green points and -13% for the orange points and their corresponding standard deviations were 43% and 54%. The frequency of occurrence of Z_{DR} versus Z_H derived from 9 RHI scans are shown in Figure 8 together with the same scattering calculations using the two methods. The drop-by-drop calculations are once again seen to be in better agreement with the radar data.

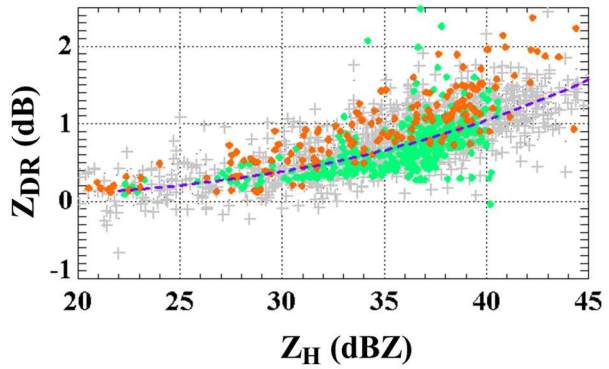

Fig. 7: Z_H versus Z_{DR} variations from Fig. 6 and power-law fitted equation to the radar data

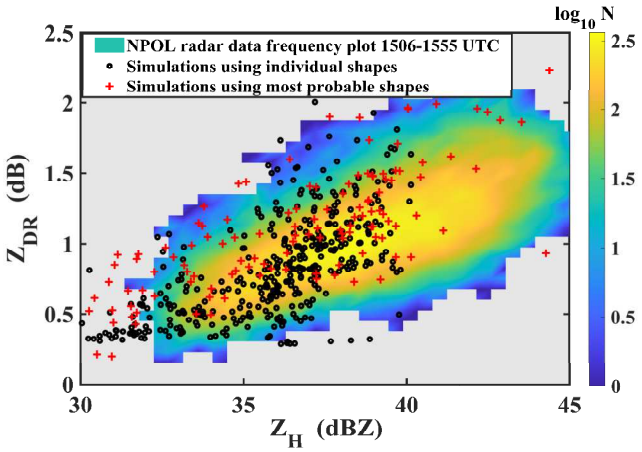

Fig. 8: Z_{DR} versus Z_H from NPOL data (frequency of occurrence in color) and the 3-minute DSD based calculations from the two methods.

V. DISCUSSION AND CONCLUSIONS

Comparison of RB values relating Fig. 7, together with the comparisons presented in Fig. 8, clearly show that the scattering calculations using individual drop shapes are significantly closer to the (calibrated) radar data than those using the equilibrium or the most probable shapes. The latter overestimates the Z_{DR} considerably. The main implication is that for this Hurricane (rain-bands) event, a significant fraction of the (> 2 mm) drops deviate from the most probable shape, tending towards sphericity. Large amplitude mixed mode oscillations are very likely to be responsible, in particular transverse oscillation, mode (2,1). The lower than expected Z_{DR} values e.g. for Z > 35 dBZ from the NPOL data is also consistent with previous radar observations at S-band for other hurricane events [22]. One factor was thought to be to the presence of high concentration of small drops as has been previously measured in such storms [23, 24]. On the other hand, the Z_{DR} calculations shown as orange points in Figure 6(b) are based on the 'full' DSD spectra, utilizing not only 2DVD data but also data from a collocated Meteorological Particle Spectrometer [25, 26] capable of measuring drop concentrations down to 0.2 mm. In [17] where output from a particle-based microphysical method is used to compare with radar observations for this very event, the authors noted the "unknown effects of strong wind gusts of a category-1 hurricane near the surface in disturbing the most probable shapes and orientation (canting angle) of drops deduced from the 80-m fall bridge experiments", the latter being given in [10]. Furthermore, in [17], the standard deviation of the effective canting angle needed to be as high as 20° (much higher than the conventional assumption of 7–10°) "to account effectively for multi-mode oscillations due to the strong wind gusts and turbulence". In support of these points, we show in Fig. 9 the variation of single particle Z_{DR} calculated using the reconstructed drop shapes with D_{eq} for all drops > 2 mm. They are represented by the green dots. The red lines represent the ± one standard deviation (σ) for each D_{eq}. As can be seen, σ is rather large, and in fact increase with D_{eq}. The '+' points in blue represent the Z_{DR} calculations using the most probable shapes from [10].Whilst they lie within the ±σ lines, they seem closer to the upper red line.

Another interesting point to note is that ±σ increase with increasing D_{eq} implying that the drop oscillation amplitudes increase with D_{eq}. This increase has indeed been noted with both wind-tunnel observations as well as the 80-m fall experiment, for example, see [27].

Thus, such storms (often associated with significant gust) may require modified polarimetric radar retrieval algorithms for estimating rainfall rates compared with more commonly occurring rain events. The estimators will need to take into consideration the change in the overall Z_{DR}, say within a radar pulse volume, occurring as a result of large amplitude mixed-mode oscillations. (Future work will address this important issue.) The 2DVD provides important drop shape information pertinent for such applications, as has been demonstrated here. Note also that in a previous study [13] relating to rain bands of a Tropical Depression (Nate), the overall Z_{DR} was not found to vary systematically from most other events. The winds associated with the Nate event were significantly lower than the hurricane event considered here.

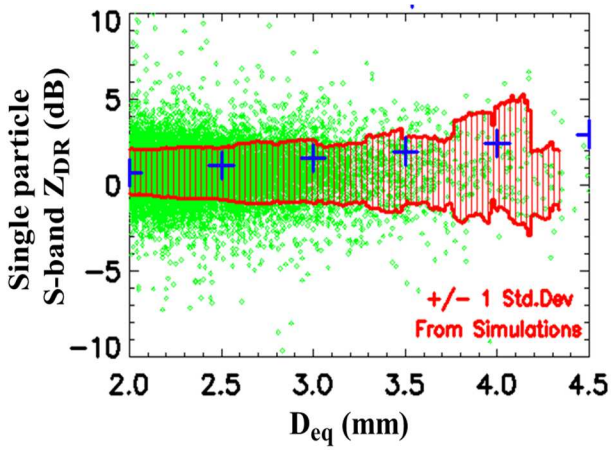

Fig. 9: Single particle Z_{DR} variation with D_{eq} calculated using reconstructed drop shapes (green dots), their ± one standard deviation (shaded red), and the expected Z_{DR} from the most probable shapes (blue + points).

Finally, as mentioned in the Introduction, drop shapes also have an impact on the XPD versus CPA variation needed for earth-space communication links [6, 7]. Data from 2DVD have been used in prior studies to simulate beacon experimental scenario and compare with actual measurements. For example in [28], simulations were carried out for the 20 GHz band and compared with beacon measurements taken in Aveiro, Portugal, over a 1-year period. Rain drop size distributions as well as the most probable shapes from [10] were used. In a later study [29], the spread in the XPD-CPA was illustrated when individual drop shape information was included. However, the individual drop shape was defined in terms of effective axis ratios (and assuming rotationally symmetry) as well as the individual orientation angle. These studies can be improved by utilizing the 3D reconstructed shapes of individual drops as well as the 3D electromagnetic analysis software packages which are now available. Note however, the XPD-CPA calculations will require complex forward scattering amplitudes for individual drops in addition to the complex backscatter amplitudes.

ACKNOWLEDGMENT

We wish to thank Prof. V. N. Bringi for helpful discussions and for providing valuable suggestions. MT received support from US National Science Foundation via grant AGS190585.

REFERENCES

[1] J. E. Allnutt, Satellite-To-Ground Radiowave Propagation, The Institution of Engineering and Technology, London, UK, 2011.

[2] T. Oguchi, "Scattering properties of Pruppacher-and-Pitter form raindrops and cross polarization due to rain: Calculations at 11, 13, 19.3 and 34.8 GHz", Radio Science, vol. 12, pp. 41-51, 1977.

[3] V. Bringi, and V Chandrasekar, Polarimetric Doppler Weather Radar: Principles and Applications, Cambridge: Cambridge University Press, UK, 2001. doi:10.1017/CBO9780511541094

[4] R. Doviak, and D. S. Zrnić, Doppler Radar and Weather Observations (Second Edition), Academic Press, 1993.

[5] S. Okamura, and T. Oguchi, "Electromagnetic wave propagation in rain and polarization effects", Proc. Japan Acad. Ser. B., Phys. Biol. Sci., vol. 86, pp. 539-562, 2010. doi: 10.2183/pjab.86.539

[6] G. Brussard, and D. V. Rogers, "Propagation considerations in satellite communication systems", Proceedings of the IEEE, vol. 78, pp. 1275-1282, 1990.

[7] A. Paraboni, A. Martellucci, C. Capsoni and C. Riva, "The physical basis of atmospheric depolarization in slant paths in the V Band: Theory, Italsat experiment and models" IEEE Transactions on Antennas and Propagation, 59, vol. 11, pp. 4301-4314, 2011. doi:10.1109/TAP.2011.2164207.

[8] A. V. Ryzhkov, and D. S. Zrnic, "Radar polarimetry for weather observations", Springer International Publishing, 2019, Switzerland.

[9] M. Szakall, S. K. Mitra, K. Diehl, and S. Borrmann, "Shapes and oscillations of falling raindrops - A Review", Atmospheric Research, vol. 97, pp. 416-425, 2010. doi: 10.1016/j.atmosres.2010.03.024

[10] M. Thurai, G-J Huang, V. N. Bringi, W. L. Randeu; and M. Schönhuber, "Drop shapes, model comparisons, and calculations of polarimetric radar parameters in rain", J. Atmos. Ocean. Technol., vol. 24, pp. 1019–1032, 2007.

[11] K. V. Beard, V.N. Bringi , and M. Thurai, "A new understanding of raindrop shape", Atmospheric Research, vol. 97, pp. 396-415, 2010.

[12] K. V. Beard and C. Chuang, "A new model for the equilibrium shape of raindrops", Journal of the Atmospheric Sciences, vol. 44, pp. 1509-1524, 1987.

[13] M. Thurai, S. Steger, F. Teschl, and M. Schönhuber, "Analysis of raindrop shapes and scattering calculations: The outer rain bands of tropical depression Nate," Atmosphere, vol. 11, pp. 114, 2020. https://doi.org/10.3390/atmos11010114

[14] S. B. Manić, M. Thurai, V. N. Bringi, and B. M. Notaroš, "Scattering calculations for asymmetric raindrops during a line convection event: Comparison with radar measurements", J. Atmos. Oceanic Technol., vol. 35, pp. 1169–1180, 2018. https://doi.org/10.1175/JTECH-D-17-0196.1.

[15] D. B. Wolff, D. A. Marks, and W. A. Petersen, "General application of the relative calibration adjustment (RCA) technique for monitoring and correcting radar reflectivity calibration", J. Atmos. Ocean. Technol. Vol. 32, pp. 496–506, 2015. doi:10.1175/JTECH-D-13-00185.1.

[16] M. Thurai, V. N. Bringi, D. B. Wolff, D. Marks, and C. S. Pabla, "Drop size distribution Measurements in outer rainbands of Hurricane Dorian at the NASA Wallops Precipitation-Research Facility", Atmosphere, vol. 11, pp. 578, 2020. doi:10.3390/atmos11060578.

[17] V. Bringi, A. Seifert, W. Wu, M. Thurai, G-J Huang, and C. Siewert, "Hurricane Dorian outer rain band observations and 1D particle model simulations: A case study", Atmosphere, vol. 11, pp. 879, 2020.

[18] M. Schönhuber, M. Schwinzerl and G. Lammer, "3D Reconstruction of 2DVD-measured raindrops for precise prediction of propagation parameters," 2016 10th European Conference on Antennas and Propagation (EuCAP), Davos, Switzerland, 2016, pp. 1-4, doi: 10.1109/EuCAP.2016.7481929.

[19] M. Schwinzerl, M. Schönhuber, G. Lammer, and M. Thurai, "3D reconstruction of individual raindrops from precise ground-based precipitation measurements," EMS Annu. Meet. Abstr. 2016, 13, EMS2016-601, Trieste, Italy, September, 2016.

[20] M. Thurai, S. Manić, M. Schönhuber, V. N. Bringi, and B. M. Notaroš, "Scattering calculations at C-Band for asymmetric raindrops reconstructed from 2D video disdrometer measurements", J. Atmos. Oceanic Technol., vol. 34, pp. 765–776, 2017. https://doi.org/10.1175/JTECH-D-16-0141.1.

[21] P. Ray, "Broadband complex refractive indices of ice and water," Appl. Opt. 1972, vol. 11, pp. 1836–1844.

[22] B. R. Brown, M. M. Bell, and A. J. Frambach, "Validation of simulated hurricane drop size distributions using polarimetric radar", Geophys. Res. Lett., vol. 43, pp. 910-917, 2016.

[23] P. T. Willis, and P. Tattelman, "Drop-size distributions associated with intense rainfall", J. Appl. Meteor., vol. 28, pp. 3–15, 1989.

[24] A. Tokay, A., P. G. Bashor, E. Habib, and T. Kasparis, "Raindrop size distribution measurements in tropical cyclones" Mon. Wea. Rev., vol. 136, pp. 1669–1685, 2008.

[25] D. Baumgardner, G. Kok, W. Dawson, D. O'Connor, and R. Newton, "A new ground-based precipitation spectrometer: The Meteorological Particle Sensor (MPS)", 11th Conf. on Cloud Physics, Ogden, Utah, USA, (Amer. Meteor. Soc.), paper 8.6., 2002.

[26] V.N. Bringi, M. Thurai, M., and D. Baumgardner, "Raindrop fall velocities from an optical array probe and 2-D video disdrometer", Atmos. Meas. Tech. vol. 11, pp. 1377-1384, 2018.

[27] M. Thurai, V.N. Bringi, M. Szakáll, S.K. Mitra, K.V. Beard, and S. Borrmann, "Drop shapes and axis ratio distributions: Comparison between 2D video disdrometer and wind-tunnel measurements", J. Atmos. Oceanic Technol., vol. 26, pp. 1427-1432, 2009.

[28] M. Thurai, V. N. Bringi, and A. Rocha, "Specific attenuation and depolarization in rain from 2-dimensional video disdrometer data", IET Microwaves Antennas Propag., vol. 1, pp. 373– 380, 2007. doi:10.1049/iet-map:20060023.

[29] M. Thurai, and V. N. Bringi, "Calculations of cross-polar discrimination spread for 20 GHz fixed satellite systems using rain microstructure information", Radio Science, vol. 44 (4), RS4006, 2009, https://doi.org/10.1029/2008RS004009.